AFCRC-TR-56-203
ASTIA DOCUMENT NO. AD-98766

GEOPHYSICAL RESEARCH PAPERS
NO. 44

LUMINOUS AND SPECTRAL REFLECTANCE AS WELL AS COLORS OF NATURAL OBJECTS

(ALBEDO AND COLOR OF TERRAIN FEATURES)

RUDOLF PENNDORF

FEBRUARY 1956

GEOPHYSICS RESEARCH DIRECTORATE
AIR FORCE CAMBRIDGE RESEARCH CENTER
AIR RESEARCH AND DEVELOPMENT COMMAND

AFCRC-TR-56-203
ASTIA DOCUMENT NO. AD-98766

GEOPHYSICAL RESEARCH PAPERS
NO. 44

LUMINOUS AND SPECTRAL REFLECTANCE AS WELL AS COLORS OF NATURAL OBJECTS

(ALBEDO AND COLOR OF TERRAIN FEATURES)

RUDOLF PENNDORF

FEBRUARY 1956

GEOPHYSICS RESEARCH DIRECTORATE
AIR FORCE CAMBRIDGE RESEARCH CENTER
BEDFORD MASSACHUSETTS

CONTENTS

ABSTRACT

The spectral reflectance of natural objects is taken from Krinov's measurements. Based on these data, the luminous reflectance (albedo) and the color parameters are computed for these objects. The results are compared with other published data.

It is shown that most natural objects possess a dominant wavelength between 5700A and 5900A, i.e. in the greenish yellow part of the spectrum. Even for vegetative formations, as seen from a distance, the dominant wavelength is also in the greenish yellow spectral range, which is a surprising fact because one would expect a dominant green. This color is, however, a mixture of brown and green.

The excitation purity of bare areas and soils is low (15-30%), but it is higher for vegetative formations (25-50%). Vertical formations such as forests, seen from directly above, reflect only a very small amount (2-3%) of the light which falls upon them from the sun and sky, but as seen from the ground their reflectance is much higher (about 8%).

LUMINOUS AND SPECTRAL REFLECTANCE

AS WELL AS

COLORS OF NATURAL OBJECTS

(VISUAL ALBEDO AND COLOR OF TERRAIN FEATURES)

1. Introduction

For many problems in atmospheric optics, the reflectance (or albedo) of natural objects is of great importance. For problems in visibility we are concerned only with the reflectance in the visible part of the spectrum, i.e. from 0.38 to 0.77 μ. Although the experimental data available are limited, they have recently been largely extended by the publication of extensive measurements of spectral reflectance of natural objects carried out in Russia. These data allow computations of luminous reflectance and color parameters. After having obtained such additional data we are in a much better position to investigate atmospheric visibility problems, such as slant visibility.

2. Definitions

By the albedo of an object we mean the fraction of the incident energy which is reflected by the body. This is a very casual definition. If we look closer at the physical process, we find that, when light is incident upon the surface of a body, some of it is, in general, directly reflected, some is diffusely reflected, while the remainder passes on into the substance of the body to be absorbed. Polished surfaces reflect directly; mat surfaces reflect diffusely.

The reflectance of a body is the ratio of the luminous flux reflected by the body to the luminous flux incident upon it. It may vary considerably with wavelength. A uniform diffusely reflecting surface may be defined as one which redistributes the radiant energy it receives in such a manner that, whatever the directional distribution of the incident radiant energy, the reflected radiant energy from each element of the surface in any given direction is proportional to the cosine of the angle which that direction makes with the normal to the surface. Such a surface, therefore, appears equally bright in all directions. Natural surfaces do not behave as an ideal diffusely reflecting surface and the simple cosine law is not accurately followed. The reflectance is greater in the neighborhood of specular reflection.

If we measure the reflectance within narrow wavelength ranges, i.e. we measure the spectral reflectance r_λ the measurements have to be defined in radiometric units. If we consider, however, the reflectance for visibility problems, it has to be defined in photometric units. We use luminous reflectance R as the important parameter, which can be computed from the spectral reflectance r_λ using the relative spectral luminosity of the human eye.

This terminology avoids the term albedo, which is more or less understood to comprise the Reflectance for the total wavelength range of the solar radiation from the ultraviolet to the far infrared. The term "visual albedo", however, is equivalent to luminous reflectance.

3. Spectral Reflectance of Natural Objects After Krinov

3.1 Method of Observation

The data we will investigate thoroughly are those obtained by Krinov.[2] He has collected an extremely large amount of data, the largest available in the literature, and his publication is available in a good translation.

His objective was to determine the spectral reflectance of natural formations, mostly plants. In the case of horizontal surfaces (for instance soil) the spectrograph was placed on a tripod and directed vertically (pointed to the nadir) or at an angle of 45° and an azimuth of 90° from the sun. In taking the spectrograms of natural formations having vertical surfaces, such as trees, the spectrograph was placed horizontally and at an azimuth of about 135° or 225° from the sun. In this case the sun was always behind and somewhat to the side of the observer (spectrograph) to give the greatest illumination (irradiance, to be correct).

Measurements were obtained on clear days and only rarely up to a cloudiness of 0.3. In cases of broken low clouds, spectrograms were taken only when the sun was shining directly at the object. Furthermore, most of the data are obtained around noon. Unfortunately, only two aircraft measurements have been successfully carried out. The open airplane was flying at 900 ft. near Leningrad. Data for two natural objects were derived: a mature fir forest and a dry meadow with low sparse grass. They will be discussed in Section 3.4.

In taking the spectrograms the procedure was to take one of the natural object and one of a standard surface within a short time interval. The spectrogram from the standard surface is necessary to determine accurately the spectral reflectance of the natural object. The reflectance of the standard surfaces was compared with that of processed magnesium oxide powder; thus, his standardization procedure was correct. The Mgo surface is the best standard, but could not be used in field work. The procedure used by Krinov was such that he must have obtained very reliable data. From his description I have the impression that the field work was carried out very carefully. We will see that our evaluation of his data leads to reliable information, when compared with results obtained by other research groups.

All in all, 10,316 spectrograms were taken on 905 plates. His work started in 1932 and continued until 1937. In 1942 additional spectra were taken. His data cover the range 4000-6500Å and a substantial amount the range 7100-9000Å.

3.2 Grouping of Krinov's Observations

This wealth of data has been worked up into 370 groups of objects, most of which are types of trees and shrubs at various seasons of the year. This might be of importance for camouflage purposes, but it certainly is not for general visibility problems. Of interest to us is only his assembly of the data into four main classes or eleven types. These eleven types characterize most of the terrain features. They are described in the next section in detail.

3.3 Results for Ground Measurements

The results of the spectral reflectance r_λ of his eleven types are given in Table 1. For some types Krinov approximated the change of r with wavelength by writing

$$r_\lambda / r_{\lambda_o} = \gamma,$$

where r_λ is the value at $\lambda = 6500 \mathring{A}$ and $\lambda_o = 4000 \mathring{A}$. The value γ is also listed in Table 1. Furthermore, the data are shown in Fig. 1a-c These are Krinov's basic data which we will use later on. We shall describe his results for the eleven types in a classification system which stems from Table 3 (discussed in Section 4).

Class A. Water surfaces (Fig. 1a): The curve has a steep negative slope in the blue part and a very gradual slope in the red portion; $\gamma = 0.19$, r_λ varies between 0.15 and 0.008. Typical examples are water surfaces at a relatively large angle from the vertical, i.e. reflecting the blue sky.

Class B. Bare areas and soils (Fig. 1b): Curve 1a represents fresh fallen snow. The r_λ values fall off gradually towards the red; $\gamma = 0.88$, the r_λ values are very high. Curve 1b represents snow covered with a film of ice. The reflectance is more or less neutral, i.e. independent of wavelength and r_λ is high, 0.72 to 0.76. Curve 2 is characteristic for limestone, clay and similar bright objects. The curve for r_λ is convex with a steep upward slant; r_λ is relatively high ($r_\lambda = 0.357$ to 0.753) with $\gamma = 1.95$.

Typical examples for curve 5 are sands, various bare areas in the desert, some mountain outcrops. The r_λ values increase rapidly from the blue to $6000 \mathring{A}$; above $6000 \mathring{A}$ the increase is only slight; $\gamma = 2.71$. Typical examples for curve 7b are podzol, clay, loam and other soils, paved roads and some buildings. The r_λ values increase slowly up to $6500 \mathring{A}$, but beyond $6500 \mathring{A}$ a steep increase is observed to large infrared values; $\gamma = 1.67$.

In the final curve, 8c, the r_λ values increase more or less uniformly towards the red end of the spectrum; $\gamma = 1.64$. Typical examples of this type are black earth, sand loam, and earth roads.

Table 1--Spectral reflectance of natural objects as measured by Krinov

Class	A	B							C		
Type λ in Å	3	1a	1b	2	5 6a	7b 8a	8c	1a	1b 3a 4	1c 3b	1d 5
4000	0.150	0.830	0.720	0.357	0.118	0.064	0.022	0.017	0.033	0.039	0.051
4100	0.130	0.828	0.722	0.378	0.116	0.065	0.022	0.017	0.034	0.041	0.053
4200	0.118	0.825	0.725	0.402	0.122	0.065	0.023	0.017	0.036	0.042	0.056
4300	0.108	0.823	0.728	0.430	0.133	0.066	0.023	0.018	0.038	0.044	0.060
4400	0.100	0.821	0.730	0.453	0.142	0.067	0.023	0.018	0.040	0.046	0.061
4500	0.091	0.820	0.733	0.475	0.150	0.068	0.023	0.018	0.041	0.048	0.062
4600	0.088	0.815	0.735	0.494	0.158	0.070	0.023	0.018	0.042	0.050	0.064
4700	0.082	0.810	0.738	0.514	0.164	0.072	0.024	0.018	0.044	0.052	0.069
4800	0.079	0.806	0.740	0.530	0.172	0.073	0.025	0.017	0.046	0.052	0.076
4900	0.074	0.800	0.741	0.545	0.178	0.075	0.025	0.017	0.047	0.054	0.079
5000	0.070	0.798	0.743	0.558	0.186	0.077	0.026	0.016	0.050	0.060	0.083
5100	0.066	0.795	0.744	0.572	0.194	0.079	0.026	0.019	0.055	0.069	0.091
5200	0.062	0.790	0.745	0.585	0.202	0.081	0.026	0.024	0.063	0.085	0.112
5300	0.060	0.785	0.746	0.598	0.211	0.084	0.027	0.027	0.075	0.108	0.134
5400	0.058	0.780	0.747	0.609	0.221	0.087	0.028	0.031	0.083	0.124	0.151
5500	0.054	0.775	0.748	0.622	0.232	0.090	0.029	0.031	0.088	0.134	0.168
5600	0.051	0.770	0.749	0.632	0.242	0.091	0.030	0.031	0.088	0.132	0.178
5700	0.048	0.765	0.750	0.640	0.252	0.092	0.030	0.031	0.084	0.123	0.191
5800	0.045	0.760	0.751	0.649	0.262	0.094	0.030	0.028	0.080	0.113	0.193
5900	0.042	0.758	0.753	0.659	0.269	0.096	0.030	0.027	0.078	0.106	0.196
6000	0.040	0.756	0.765	0.667	0.273	0.098	0.030	0.028	0.078	0.101	0.196
6100	0.035	0.750	0.766	0.675	0.276	0.100	0.031	0.026	0.080	0.096	0.191
6200	0.032	0.748	0.757	0.682	0.279	0.101	0.033	0.026	0.079	0.093	0.193
6300	0.030	0.745	0.758	0.687	0.281	0.103	0.034	0.027	0.079	0.088	0.193
6400	0.029	0.740	0.759	0.692	0.282	0.105	0.035	0.026	0.078	0.085	0.190

Table 1 - (Continued)

Class	A	B						C			
Type λ in Å	3	1a	1b	2	5 6a	7b 8a	8c	1a	1b 3a 4	1c 3b	1d 5
6500	0.027	0.735	0.760	0.697	0.281	0.107	0.036	0.022	0.077	0.084	0.193
6600	0.025	0.730	0.760	0.700	0.283	0.115	0.037	0.023	0.077	0.084	0.212
6700	0.021	0.725	0.760	0.704	0.284	0.124	0.038	0.027	0.084	0.095	0.234
6800	0.020	0.720	0.760	0.709	0.286	0.132	0.039	0.033	0.099	0.113	0.259
6900	0.018	0.715	0.760	0.712	0.288	0.142	0.040	0.042	0.116	0.142	0.285
7000	0.017	0.710	0.760	0.718	0.290	0.165	0.041	0.059	0.140	0.176	0.315
7100	0.015	0.705	0.760	0.721	0.292	0.169	0.042	0.078	0.167	0.222	0.345
7200	0.014	0.700	0.760	0.723	0.295	0.179	0.043	0.099	0.189	0.268	0.378
7300	0.013	0.695	0.760	0.727	0.299	0.189	0.044	0.119	0.209	0.318	0.409
7400	0.012	0.690	0.760	0.730	0.302	0.196	0.045	0.132	0.225	0.360	0.443
7500	0.011	0.685	0.760	0.732	0.306	0.204	0.046	0.144	0.239	0.397	0.460
7600	0.010	0.680	0.760	0.736	0.309	0.208	0.047	0.152	0.251	0.429	0.481
7700	0.010	0.675	0.760	0.738	0.312	0.216	0.048	0.162	0.272	0.455	0.500
7800	0.010	0.670	0.760	0.740	0.316	0.225	0.050	0.167	0.278	0.480	0.518
7900	0.009	0.660	0.760	0.742	0.319	0.236	0.053	0.170	0.282	0.507	0.528
8000	0.009	0.655	0.760	0.744	0.318	0.244	0.059	0.172	0.284	0.516	0.540
8100	0.008	0.650	0.760	0.748	0.324	0.252	0.061	0.178	0.287	0.528	0.549
8200	0.008	0.640	0.760	0.750	0.331	0.256	0.065	0.181	0.290	0.538	0.555
8300	0.008	0.635	0.760	0.752	0.336	0.264	0.069	0.184	0.294	0.536	0.561
8400	0.008	0.630	0.760	0.753	0.341	0.270	0.071	0.189	0.305	0.542	0.564
Y	0.19	0.88	–	1.95	2.71	1.67	1.64	–	–	–	–

Class C. Vegetative formations (Fig. 1c): Type 1a: The curve has a very weak maximum in the visible region of the spectrum and, in general, the r_λ values are very small. In the red part of the spectrum the r_λ show an upward sloping. Typical examples are coniferous forests in winter.

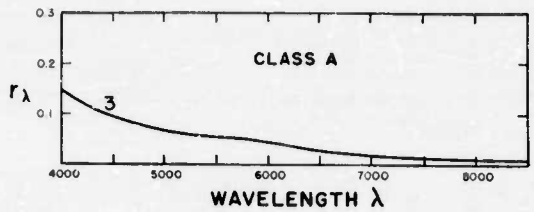

Fig. 1a

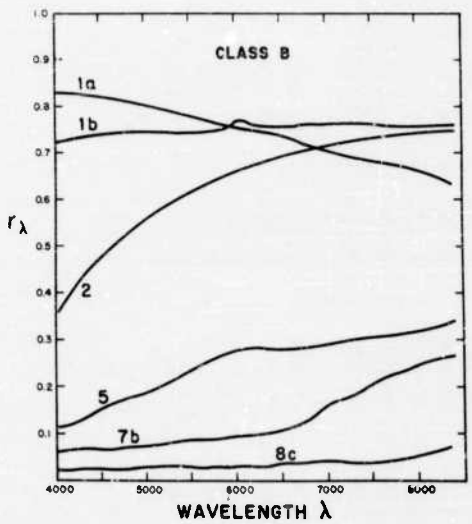

Fig. 1b

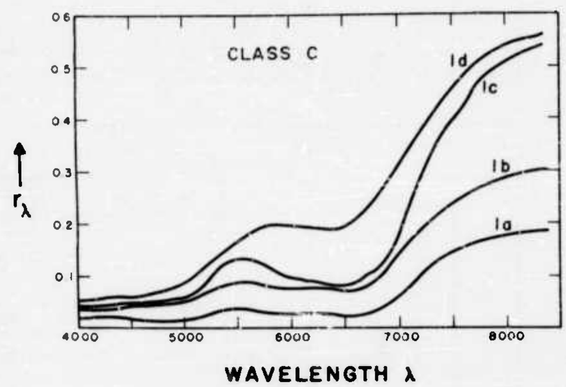

Fig. 1c

Fig. 1. Spectral reflectance for eleven types of natural objects as measured by Krinov.

a) For Class A: Water surfaces

b) For Class B: Bare areas and soils

c) For Class C: Vegetative formations

The numbers on the curves correspond to those in Table 3 and in the text.

Type 1b: The curve has a more distinct maximum in the visible region of the spectrum and is higher than the previous curve. Furthermore, it possesses the same noticeable upward slant in the near infra-red region. Typical examples are coniferous forests in the summer period, dry meadows and grass in general, excluding lush grass.

Type 1c: The curve has a clearly expressed maximum in the yellow-green region of the spectrum and a very strong upswing in the infrared region. Typical examples are deciduous forests in the summer period and all lush grass.

Type 1d: The curve has an upward slant in the entire green-orange-red portion of the spectrum, and a steep slope in the red-infrared spectrum. Typical examples of this type are forests in the autumn period and ripe field crops.

3.4 Results for Airplane Measurements

Of importance to our basic problem are those spectrograms taken from low flying airplanes. There exist only few data in the open literature, namely those obtained by Krinov and those by Schimpf and Aschenbrenner.*[7] The later ones used a Titanium dioxide surface for comparison. The results are listed in Table 2 and reproduced in Fig. 2. Krinov flew at 300 m (900 ft.) near Leningrad; Schimpf and Aschenbrenner near Berlin (Germany) at 100 m (300 ft.). Both flew over similar terrain features and therefore their results can be compared. The results do not quite agree numerically because the time of the year, the position of the sun, the density of the forest or grass were probably different. But the type of curves obtained for r_λ is very similar, as seen from Fig. 2. It might be possible that Krinov's airplane data for both objects are a bit larger than Schimpf and Aschenbrenner's, because they contain a larger contribution from the air-light. But this can only be proven by computing the influence of airlight on luminance, for a layer 200 m thick.

* The original article is not available, and the data have been taken from a publication by Nagel.[6]

Table 2--Spectral reflectance r_λ for low flying airplane

λ in Å	Mature fir forest, late su. Krinov, 300 m.	Forest, su. Schimpf, Aschenbrenner, 100 m.	Meadow, low dense grass early fall Krinov 300 m.	Meadow Schimpf, Aschenbrenner, 100 m.
4000	0.030	0.011	0.054	0.023
4100	.026	.015	.050	.029
4200	.026	.017	.050	.032
4300	.026	.016	.048	.035
4400	.025	.019	.050	.039
4500	.024	.020	.047	.040
4600	.024	.016	.047	.041
4700	.025	.018	.047	.044
4800	.025	.019	.046	.044
4900	.025	.017	.050	.045
5000	.025	.017	.051	.049
5100	.027	.020	.057	.055
5200	.030	.023	.067	.060
5300	.034	.024	.077	.068
5400	.036	.026	.085	.076
5500	.038	.026	.091	.078
5600	.036	.026	.094	.078
5700	.035	.025	.089	.076
5800	.031	.023	.083	.072
5900	.030	.023	.085	.072
6000	.028	.023	.087	.075
6100	.030	.023	.083	.072
6200	.028	.023	.080	.068
6300	.027	.022	.079	.063
6400	.026	.021	.075	.059
6500	.028	.020	.075	.058
6600		.023		.058
6700		.024		.055
6800		.024		.050
6900		.022		.047
7000		.022		.046

First we compare the spectral reflectance of meadows. As we see from Fig. 2a, the results of Krinov, and Schimpf and Aschenbrenner, from an airplane, agree fairly well with those obtained by Krinov from the ground.* This leads to the conclusion that Krinov's data, measured near the ground, can be applied for visibility problems from aircraft (slant visibility) as long as bare areas, soils and shallow or dense vegetative formations are concerned.

Quite contrary are the results for fir forests. Here the r_λ values obtained by both authors from airplanes agree more or less, but the values are substantially lower than those obtained from the ground looking horizontally at a forest. The reflectance for an airplane observer is only ½ to ¼ of that for a ground

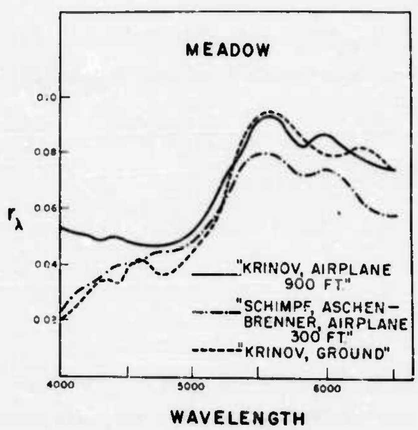

Fig 2a

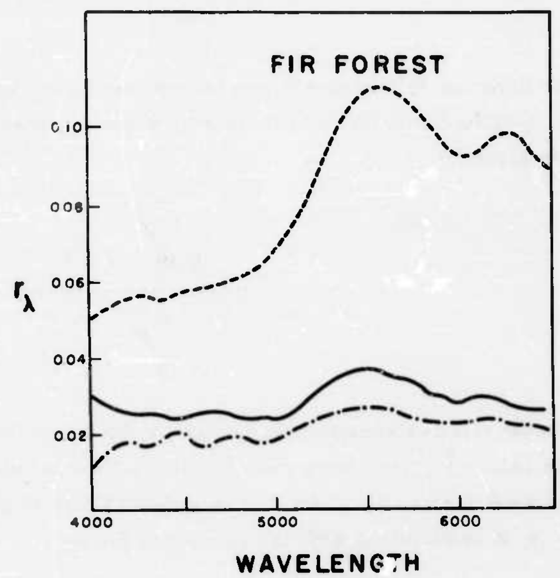

Fig. 2b

Fig. 2. Spectral reflectance of meadows and fir forests as measured from low flying aircrafts.

a) For meadows

b) For fir forest

The ground values for the same objects are also entered after Krinov.

*The "ground" values of r_λ in Fig. 2a and 2b are data taken from an individual observation of the same object at the same time of year; they are not average data taken from Table 1.

observer as seen from Fig. 2b. It is caused by the large shadow areas between the individual trees. The conclusion is that vertical vegetative formations, like forests and shrubs with no solid upper leaf surface possess a substantially lower spectral reflectance for an airplane observer looking vertically down as compared with a ground observer. The reflectance should increase somewhat for slant visibility.

4. Luminous Reflectance of Natural Objects

4.1 Computation for Krinov's Types of Natural Objects

The luminous reflectance R can be computed from data of r_λ. If H_λ is the spectral irradiance of the surface for specified angular conditions of irradiance,* then the luminous reflectance R of non-fluorescent materials is given by

$$R = \frac{\int_{0.38}^{0.77} r_\lambda \bar{y}_\lambda H_\lambda \, d\lambda}{\int_{0.38}^{0.77} \bar{y}_\lambda H_\lambda \, d\lambda}$$

where $\bar{y}_\lambda$ is the relative spectral luminosity for the human eye at a specific level of luminance. For bright daylight the values $\bar{y}_\lambda$ have been published for a "normal observer," they correspond to CIE, standard source B. The values R are computed for Krinov's data (Table 1) together with the chromaticity coordinates in Section 5, i.e. R is identical with the luminance factor Y.

4.2 Other Available Data

There exist two other sets of data. One is published in the Smithsonian Meteorological Tables[3] where data from many investigators are neatly summarized, and one set in Sewing's handbook.[8] All those R values are based on aircraft measurements, as stated in the text to these tables, and thus we can compare most of them with our computations, based on Krinov's measurements, provided the conclusions in Section 3.4 are valid.

---

* In this case CIE standard source B, see Section 5.1.

4.3 Comparison of Data

In order to compare the data, a list has been set up (Table 3) in which all four sets of data are listed, but we cannot compare all the data, because they are not taken under the same conditions. The descriptive terms follow the usage of the individual authors. We can now classify the results in four classes. Natural objects (Class A, B) have, in general, very low or very high values of luminous reflectance. While snow, sand and some rocks have R values ranging from 30 to 90%, water surfaces and bare ground have values of 5-10%. Vegetative formations (Class C) also show small values, mostly below 10%. The differences within the later class are slight and on this basis hard to distinguish; thus, color contrast can help to distinguish the objects. The difference between dry and wet soil conditions is striking; wet conditions always reduce R. Different types of roads and buildings (Class D) show a large variation of R.

The Smithsonian Tables list R values giving lower and upper boundaries. Sewing's table, as well as our computations based on Krinov's or Schimpf-Aschenbrenner's r_λ values, list only one value, but limits should be added which could be obtained from Krinov's data. This, however, requires laborious computations The figures should be considered as an indication of the approximate value and ± 50% might be a good guess of the actual variations under natural conditions.

5. Colors of Natural Objects

5.1 Method of Computing Colors

Natural objects can easily be distinguished by colors, but their colors change when viewed from increasing distances. We shall investigate here only the color of selected natural objects for an observer close to the object, i.e. we neglect the influence of airlight on colors, because this demands a separate careful study and some results are already available [4,5]

Color is certainly an intriguing subject and not easy to assess in pure physical terms, because the parameters we will compute define only the stimulus in terms of the eye, but not the mental perception this stimulus will produce. It must be remembered that luminance is one of the most important variables of color. This is easily understood, if we think of the photographic analogue "black and white," i.e. a photographic picture is essentially based only on luminance contrast of objects and perfectly understood by our minds without any real "color." Even in color photography luminance contrast is the most important variable. The same analogue applies to visibility problems. Some natural objects are exposed to bright sunshine, others or at least parts of other objects are situated in the shadow; some shine very brightly, while others don't.

We follow the standard procedure[1] in computing the various color parameters. The color of an object, reflecting light which falls upon it, depends on the spectral reflectance r_λ of this object, on the irradiance

Table 3--Luminous reflectance R in percent

		Smithsonian Tables	Sewing Handbook	Krinov	Schimpf, Aschenbrenner
Class: A	Water Surfaces				
1	Bay	3 - 4			
2	Bay and river	6 - 10			
3	Inland water	5 - 10		5	
4	Ocean	3 - 7			
5	Ocean, deep	3 - 5			
Class: B	Bare areas and soils				
1a	Snow, fresh fallen	70 - 86		77	
1b	" , covered with ice			75	
2	Limestone, clay			63	
3	Calcareous rocks		30		
4	Granite		12		
5	Mountain tops, bare			24	
6a	Sand, dry		31	24	
6b	" , wet		18		
7a	Clay soil, dry		15		
7b	" " , wet		7.5	9	
8a	Ground, bare, rich soil, dry	10 - 20	7.2	9	
8b	" " " " , wet		5.5		
8c	" , black earth, sand loam			3	
8d	Field, plowed, dry	20 - 25			
Class: C	Vegetative Formations				
1a	Coniferous forest, winter			3	
1b	" " , summer	3 - 10		8	
1c	Deciduous forest, summer			10	
1d	" " , fall			15	
1e	Dark hedges		1		
2	Coniferous forest, summer, from airplane			3	2
3a	Meadow, dry; grass	3 - 6		8	
3b	Grass, lush	15 - 25		10	
4	Meadow, low grass, from airplane			8	7
5	Field crops, ripe	7		15	
Class: D	Roads and Buildings				
1	Earth roads			3	
2	Black top roads		8	9	
3a	Concrete road, smooth, dry		35		
3b	" " " , wet		15		
4a	" " , rough, dry		35		
4b	" " " , wet		25		
5	Buildings			9	
6	Limestone tiles		25		

$H_\lambda\, d\lambda$ in the wavelength interval $\lambda \pm 1/2\, d\lambda$ at the surface of the object and on the tristimulus values $\bar{x}_\lambda$, $\bar{y}_\lambda$, $\bar{z}_\lambda$ of the human eye of a standard observer with normal color perception:

$$X = \int H_\lambda\, r_\lambda\, \bar{x}_\lambda\, d\lambda\,,$$
$$Y = \int H_\lambda\, r_\lambda\, \bar{y}_\lambda\, d\lambda\,,$$
$$Z = \int H_\lambda\, r_\lambda\, \bar{z}_\lambda\, d\lambda\,.$$

These are the tristimulus values X, Y, Z. The chromaticity coordinates are then given by

$$x = \frac{X}{X+Y+Z}\,, \qquad y = \frac{Y}{X+Y+Z}\,, \qquad z = \frac{Z}{X+Y+Z}\,.$$

They are best represented in the (now standard) chromaticity diagram,[1,4] a practice we shall follow. Since $x + y + z = 1$, only x and y need to be given to represent a chromaticity. Y gives the luminance factor directly in percent, this is accomplished by proper normalization of the $H_\lambda\, \bar{x}_\lambda$, $H_\lambda\, \bar{y}_\lambda$ and $H_\lambda\, \bar{z}_\lambda$ values. This luminance factor Y is identical with the luminous reflectance R, as given in Table 3.

Thus, the chromaticity coordinates can express the luminance factor (Y) (or R) as well as the chromaticity of an object. Further helpful parameters are the dominant wavelength λ_d, and the excitation purity p. Dominant wavelength indicates what part of the spectrum has to be mixed with the neutral standard and purity indicates the degree of approach of the color of the object to the pure spectrum color. All these parameters will be computed.

The selection of the best standard source has to be decided. Source B represents noon conditions on a clear day, whereas Source C represents average daylight, such as under an overcast sky. Source C is generally used in this country for the computation of color coordinates from photometric data.

Source B was preferred for various reasons. First of all, Krinov measured only on clear days around noon and we shall use his original data; secondly, we shall apply our results later on to problems in atmospheric visibility (slant visibility) and shall consider clear sky conditions too; thirdly, convenient tables are available.

The last remaining problem is to decide the chromaticity, which is being considered as "white". This is not necessarily or even usually the equal energy point, but rather the color of the general illumination prevailing. Thus, we consider as pure white the point of our standard Source B on the chromaticity diagram. A chromaticity diagram is shown in Fig. 3.

5.2 Colors for Krinov's Types of Natural Objects

The results of the computations are listed in Table 4 and shown in Fig. 4, where only a small portion of the chromaticity diagram is reproduced.* Only a few dominant wavelengths are indicated. The chromaticity coordinates of the CIE standard source B are: $x = 0.3485$ and $y = 0.3518$.

---

* To familiarize the reader with the chromaticity diagram, Fig. 3 shows the full chart. The two areas, which are shown enlarged as Fig. 4 and Fig. 5, are indicated on this chart.

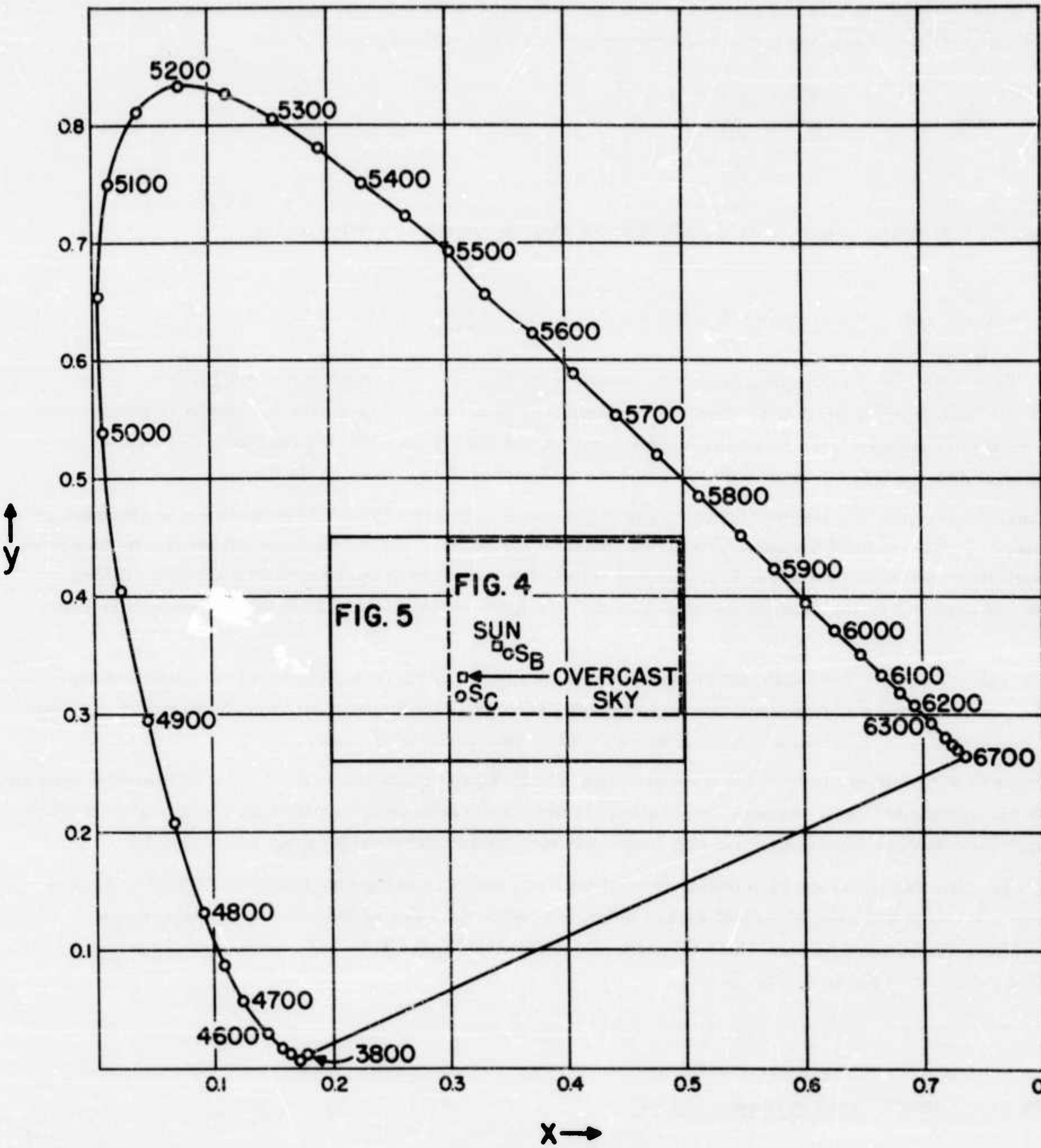

Fig. 3. **Key diagram showing regions of the chromaticity diagram displayed in Figure 4 and Figure 5.**

The chromaticity diagram is the right angle type. x = red, y = green, the third coordinate z (blue) = 0 runs at 45° through $x = 0$, $y = 1.0$ and $x = 1.0$ and $y = 0$. The full line represents the chromaticities of the spectrum identified by wavelength in A, i.e. for purity $p = 100\%$. For any point F (x,y) the line between the standard source B and this point crosses the spectrum locus at D which gives λ_d . The ratio of the distances determines the purity $p = BF/BD$.

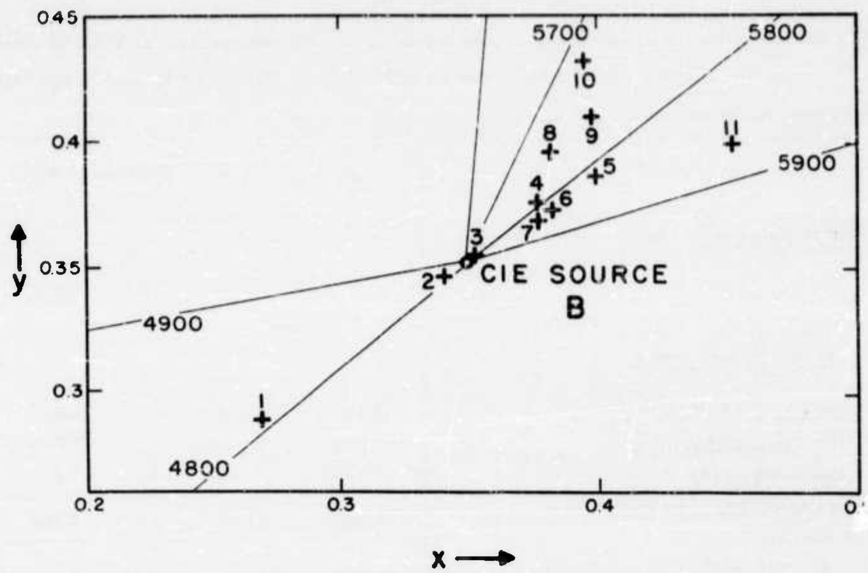

Fig. 4. Apparent chromaticity of natural objects, using Krinov's basic data of the spectral reflectance r_λ. For CIE standard source B.

Water seen at a large angle from the vertical appears blue, the dominant wavelength is 4810A and the purity 31%. These values agree with the color of the blue sky (for global irradiance) and they compare well with Moeller's data for the color of a wall exposed to global irradiance from the sun and sky.

Snow appears as a pure white surface, because a purity of 2 or 3% may be just a computational result and for practical considerations we can assume a value of p = 0%, i.e. pure white. This result is, of course, what we expect, but it serves as a check on the reliability of the basic measurements carried out by Krinov.

For all other objects the dominant wavelength varies between 5700 and 5900Å, i.e. it is restricted to a relatively narrow band in the spectrum and can be described as ranging from greenish yellow to yellowish orange. Such a result is expected for bare areas and soils; their purity is low, namely 15-30%. But this dominant wavelength is rather surprising for all vegetative formations, where a more greenish color is expected. For those the purity is relatively high, 25-50%. Unfortunately, we have no other experimental data to check those results. Moeller obtained for a green leaf, using basic measurements by Sauberer, λ_d = 5100Å, Y = 4% and p = 23%. Thus Moeller obtained a real green color. But the results listed in Table 4 may be understood as those of the total appearance of a forest or a meadow and not as valid for a part of it, like a green leaf. Krinov measured from a distance and a forest consists of green leaves, brown or nearly black branches, tree trunks and also some soil. Therefore, Krinov's colors are caused by a mixture of all those components and should be understood as such. The purity reaches its lowest value for a coniferous forest in winter and the values increase the more dominant one object becomes in the total appearance of the formation, for example, for a meadow of lush grass.

The influence of our selection of the standard source has been investigated too. For #9, coniferous forests in summer and meadows, the chromaticity coordinates have been calculated for the CIE standard source C, and the results are:

$$x = 0.362, \quad y = 0.385, \quad Y = 8\% \quad \lambda_d = 5740A, \text{ and } p = 38\%.$$

Table 4. Characteristic values of chromaticity coordinates x, y; luminance factor Y in %; dominant wavelength λ_d; and excitation purity p in % for natural object, based on Krinov's spectral reflectance data for standard source B.

#			x	y	Y in %	λ_d	p in %
	Class A:	Water Surfaces					
1	3	Inland water	0.269	0.289	5	4810	31
	Class B:	Bare areas and soils					
2	1a	Snow, fresh fallen	0.340	0.346	77	4810	5
3	1b	" , covered with ice	0.351	0.354	75	5795	2
4	2	Limestone, clay	0.377	0.376	63	5790	18
5	5 6a	Mountain tops, bare Sand, dry	0.399	0.387	24	5816	29
6	7b 8a	Clay, soil, wet Ground, bare, rich soil, dry	0.382	0.373	9	5828	18
7	8c	" , black earth, sand, loam	0.377	0.369	3	5832	15
	Class C:	Vegetative Formations					
8	1a	Coniferous forests, winter	0.381	0.396	3	5744	25
9	1b 3a	" " , summer Meadow, dry; grass	0.397	0.410	8	5758	36
10	1c 3b	Deciduous forest, summer Grass, lush	0.394	0.432	10	5719	43
11	1d 5	Deciduous forests, fall Field crops, ripe	0.451	0.399	15	5858	50
	Class D:	Roads and Buildings					
7	1	Earth roads	0.377	0.369	3	5832	15
6	2 5	Black top roads Buildings	0.382	0.373	9	5828	18

A comparison of these figures with those for the same object in Table 4 shows that, although the chromaticity coordinates are different (this is caused by the different standard source), the dominant wavelength and the purity are practically equal for both sources. Thus it is concluded that the influence of our selection of the CIE standard source on λ_d and p is of minor importance, and λ_d and p are for a first approximation valid for clear as well as overcast sky.

5.3 Colors for Natural Objects as Seen From Low Flying Airplanes

For our problem of slant visibility from aircraft, we have to use color parameters measured from low flying airplanes, to exclude the influence of airlight. Since only a few data are available, namely from

Krinov[2] and Schimpf-Aschenbrenner,[7] we investigate both of them to see how reliable the bulk of Krinov's measurements are (namely those carried out close to the ground).

The basic data (i.e. r_λ) for meadows and forests are available in Table 2, from which we computed the color parameters. The results are listed in Table 5 and represented in a chromaticity diagram in Fig. 5.

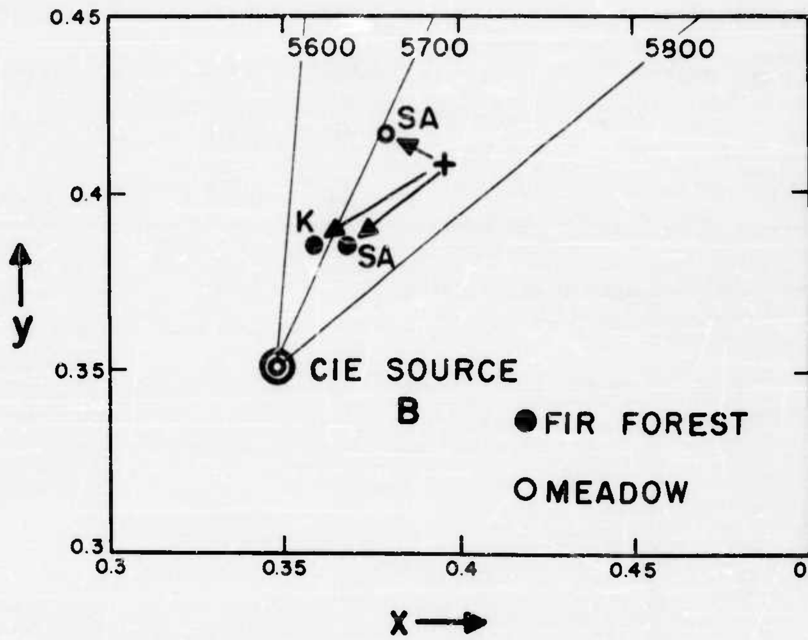

Fig. 5. Apparent chromaticity for meadow and fir forest as seen from a low flying aircraft.

SA = Schimpf-Aschenbrenner

K = Krinov

\+ values from ground after Krinov

For meadows there exists practically no difference in the color parameters as measured from a low flying airplane or as measured near the ground. The values of x, y, Y, λ_d and p are for practical purposes the same. But, quite the contrary is true for coniferous forests. The luminance factor Y (= luminance reflectance R) is reduced by 1/3 to 1/4 if seen directly from above a forest instead of horizontally from the ground. This effect is caused mostly by the large shadow areas. Thus, coniferous forests may be treated as black targets for many practical problems. Furthermore, the dominant wavelength is shifted a bit towards shorter wavelengths, i.e. from the greenish yellow to the yellow green and a very striking reduction of the purity occurs, it decreases from 36% to 18-22%, i.e. by a factor of about 1/2.

Thus, we can conclude that Krinov's measurements from the ground can be faithfully used to give colors as seen from an airplane, as long as horizontal natural objects are concerned, namely bare areas, soils, meadows, roads, lakes and rivers; but his values cannot be used for vertical natural objects like forests or buildings. In such cases individual measurements have to be carried out from low flying airplanes.

Table 5. Characteristic values of chromaticity coordinates x, y; luminance factor Y in %, dominant wavelength λ_d and excitation purity p in % for natural objects as seen from low flying airplanes and from the ground (Standard Source B).

	x	y	Y	λ_d	P
Deciduous forest ground (K)	0.397	0.410	8	5758	36
Deciduous forest airplane (K)	0.359	0.385	3	5665	22
Deciduous forest airplane (SA)	0.368	0.385	2	5719	18
Meadow, ground (K)	0.397	0.410	8	5758	36
Meadow airplane (SA)	0.380	0.417	7	5700	32

(K = Krinov; SA = Schimpf and Aschenbrenner)

REFERENCES

1. Judd, D.B., Color in Business, Science and Industry, J. Wiley and Sons, Inc., New York (1952).

2. Krinov, E.L., Spectral Reflectance Properties of Natural Formations (in Russian, 1947). National Research Council of Canada Technical Translation TT-439, Ottawa, 1953.

3. List, R.J., Smithsonian Meteorological Tables, rev. ed., 6, 442-443, Smithson. Inst. Washington, D.C. (1951).

4. Middleton, W.E.K., Vision Through the Atmosphere, Univ. of Toronto Press, Toronto (1952).

5. Moeller, F., "Ueber die Farbe der Sicht und des Tageshimmels," Arch. Met., Geophys, und Bioklimat., B. 5, 1 (1953).

6. Nagel, M., "Ueber die spektrale Energieverteilung im Mattscheibenbilde einer von Sonne, Himmel und Reflexlicht beleuchteten Kugel," Optik 6, 358 (1950).

7. Schimpf, R. and C. Aschenbrenner, "Untersuchungen ueber die spektrale Zusammensetzung der bei Luftaufnahmen wirksamen Strahlung," Zs. f. angew. Photogr. 2, 41 (1940).

8. Sewing, R., Handbuch der Lichttechnik, J. Springer, Berlin (1938).

GEOPHYSICAL RESEARCH PAPERS

No. 1. Isotropic and Non-Isotropic Turbulence in the Atmospheric Surface Layer, Heinz Lettau, Geophysics Research Directorate, December 1949.

No. 2. Effective Radiation Temperatures of the Ozonosphere over New Mexico, Adel, Geophysics R-D, December 1949.

No. 3. Diffraction Effects in the Propagation of Compressional Waves in the Atmosphere, Norman A. Haskell, Geophysics Research Directorate, March 1950.

No. 4. Evaluation of Results of Joint Air Force-Weather Bureau Cloud Seeding Trials Conducted During Winter and Spring 1949, Charles E. Anderson, Geophysics Research Directorate, May 1950.

No. 5. Investigation of Stratosphere Winds and Temperatures From Acoustical Propagation Studies, Albert P. Crary, Geophysics Research Directorate, June 1950.

No. 6. Air-Coupled Flexural Waves in Floating Ice, F. Press, M. Ewing, A. P. Crary, S. Katz, and J. Oliver, Geophysics Research Directorate, November 1950.

No. 7. Proceedings of the Conference on Ionospheric Research (June 1949), edited by Bradford B. Underhill and Ralph J. Donaldson, Jr., Geophysics Research Directorate, December 1950.

No. 8. Proceedings of the Colloquium on Mesospheric Physics, edited by N. C. Gerson, Geophysics Research Directorate, July 1951.

No. 9. The Dispersion of Surface Waves on Multi-Layered Media, Norman A. Haskell, Geophysics Research Directorate, August 1951.

No. 10. The Measurement of Stratospheric Density Distribution with the Searchlight Technique, L. Elterman, Geophysics Research Directorate, December 1951.

No. 11. Proceedings of the Conference on Ionospheric Physics (July 1950) Part A, edited by N. C. Gerson and Ralph J. Donaldson, Jr., Geophysics Research Directorate, April 1952.

No. 12. Proceedings of the Conference on Ionospheric Physics (July 1950) Part B, edited by Ludwig Katz and N. C. Gerson, Geophysics Research Directorate, April 1952.

No. 13. Proceedings of the Colloquium on Microwave Meteorology, Aerosols and Cloud Physics, edited by Ralph J. Donaldson, Jr., Geophysics Research Directorate, May 1952.

No. 14. Atmospheric Flow Patterns and Their Representation by Spherical-Surface Harmonics, B. Haurwitz and Richard A. Craig, Geophysics Research Directorate, July 1952.

No. 15. Back-Scattering of Electromagnetic Waves From Spheres and Spherical Shells, A. L. Aden, Geophysics Research Directorate, July 1952.

No. 16. Notes on the Theory of Large-Scale Disturbances in Atmospheric Flow With Applications to Numerical Weather Prediction, Philip Duncan Thompson, Major, U. S. Air Force, Geophysics Research Directorate, July 1952.

GEOPHYSICAL RESEARCH PAPERS (Continued)

No. 17. The Observed Mean Field of Motion of the Atmosphere, Yale Mintz and Gordon Dean, Geophysics Research Directorate, August 1952.

No. 18. The Distribution of Radiational Temperature Change in the Northern Hemisphere During March, Julius London, Geophysics Research Directorate, December 1952.

No. 19. International Symposium on Atmospheric Turbulence in the Boundary Layer, Massachusetts Institute of Technology, 4-8 June 1951, edited by E. W. Hewson, Geophysics Research Directorate, December 1952.

No. 20. On the Phenomenon of the Colored Sun, Especially the "Blue" Sun of September 1950, Rudolf Penndorf, Geophysics Research Directorate, April 1953.

No. 21. Absorption Coefficients of Several Atmospheric Gases, K. Watanabe, Murray Zelikoff and Edward C. Y. Inn, Geophysics Research Directorate, June 1953.

No. 22. Asymptotic Approximation for the Elastic Normal Modes in a Stratified Solid Medium, Norman A. Haskell, Geophysics Research Directorate, August 1953.

No. 23. Forecasting Relationships Between Upper Level Flow and Surface Meteorological Processes, J. J. George, R. O. Roche, H. B. Visscher, R. J. Shafer, P. W. Funke, W. R. Biggers and R. M. Whiting, Geophysics Research Directorate, August 1953.

No. 24. Contributions to the Study of Planetary Atmospheric Circulations, edited by Robert M. White, Geophysics Research Directorate, November 1953.

No. 25. The Vertical Distribution of Mie Particles in the Troposphere, R. Penndorf, Geophysics Research Directorate, March 1954.

No. 26. Study of Atmospheric Ions in a Nonequilibrium System, C. G. Stergis, Geophysics Research Directorate, April 1954.

No. 27. Investigation of Microbarometric Oscillations in Eastern Massachusetts, E. A. Flauraud, A. H. Mears, F. A. Crowley, Jr., and A. P. Crary, Geophysics Research Directorate, May 1954.

No. 28. The Rotation-Vibration Spectra of Ammonia in the 6- and 10-Micron Regions, R. G. Breene, Jr., Capt., USAF, Geophysics Research Directorate, June 1954.

No. 29. Seasonal Trends of Temperature, Density, and Pressure in the Stratosphere Obtained With the Searchlight Probing Technique, Louis Elterman, July 1954.

No. 30. Proceedings of the Conference on Auroral Physics, edited by N. C. Gerson, Geophysics Research Directorate, July 1954.

No. 31. Fog Modification by Cold-Water Seeding, Vernon G. Plank, Geophysics Research Directorate, August 1954.

GEOPHYSICAL RESEARCH PAPERS (Continued)

No. 32. Adsorption Studies of Heterogeneous Phase Transitions, S. J. Birstein, Geophysics Research Directorate, December 1954.

No. 33. The Latitudinal and Seasonal Variations of the Absorption of Solar Radiation by Ozone, J. Pressman, Geophysics Research Directorate, December 1954.

No. 34. Synoptic Analysis of Convection in a Rotating Cylinder, D. Fultz and J. Corn, Geophysics Research Directorate, January 1955.

No. 35. Balance Requirements of the General Circulation, V. P. Starr and R. M. White, Geophysics Research Directorate, December 1954.

No. 36. The Mean Molecular Weight of the Upper Atmosphere, Warren E. Thompson, Geophysics Research Directorate, May 1955.

No. 37. Proceedings on the Conference on Interfacial Phenomena and Nucleation.
I. Conference on Nucleation.
II. Conference on Nucleation and Surface Tension.
III. Conference on Adsorption.
Edited by H. Reiss, Geophysics Research Directorate, July 1955.

No. 38. The Stability of a Simple Baroclinic Flow With Horizontal Shear, Leon S. Pocinki, Geophysics Research Directorate, July 1955.

No. 39. The Chemistry and Vertical Distribution of the Oxides of Nitrogen in the Atmosphere, L. Miller, Geophysics Research Directorate, April 1955.

No. 40. Near Infrared Transmission Through Synthetic Atmospheres, J. N. Howard, Geophysics Research Directorate, November 1955.

No. 41. The Shift and Shape of Spectral Lines, R. G. Breene, Geophysics Research Directorate, October 1955.

No. 42. Proceedings on the Conference on Atmospheric Electricity, R. Holzer, W. Smith, Geophysics Research Directorate, December 1955.

No. 43. Methods and Results of Upper Atmospheric Research, J. Kaplan, G. Schilling, H. Kallman, Geophysics Research Directorate, November 1955.